Polymer Testing 101 (2021) 107305

Contents lists available at ScienceDirect

Polymer Testing

journal homepage: www.elsevier.com/locate/polytest

Temperature dependence of vibrational motions of thin polystyrene films by infrared reflection-absorption spectroscopy: A single measurement tool for monitoring of glass transition and temperature history

Barbora Hanulikova, Tereza Capkova *, Jan Antos, Michal Urbanek, Pavel Urbanek, Jakub Sevcik, Ivo Kuritka

Centre of Polymer Systems, Tomas Bata University in Zlin, tr. Tomase Bati 5678, 760 01, Zlín, Czech Republic

ARTICLE INFO

Keywords:
Infrared reflection-absorption spectroscopy
Polarization
Glass transition temperature
Polystyrene
Thin film

ABSTRACT

A method for monitoring of vibrational response and temperature region of glass transition by a single analysis is introduced with the use of an otherwise well-known spectroscopic method. The temperature-dependent changes of polystyrene (PS) thin films were investigated by polarization-modulated infrared reflection-absorption spectroscopy. The study revealed that changes in individual spectral regions with the temperature increase are specific and provide the relation to the processing and thermal history of the thin film. Temperature responses of infrared spectral region areas; an abrupt change of C_{ar}-H stretching, a step-like change of C_{ar}-H out-of-plane bending, a linear decrease of C–H stretching and C–H bending area, granted information on the temperature domain represented by local molecular motion change (β-transition) of PS. The different behavior of spectral regions is rationalized by consideration of vibrational free volume contribution to the total free volume of the system that is certainly influenced by functional groups nature, such as their size, geometry and involvement of non-bonding interaction.

CRediT authorship contribution statement

Barbora Hanulikova: Conceptualization, Formal analysis, Data curation, Writing – Original Draft. Tereza Capkova: Investigation, Validation, Data curation, Writing – Original Draft. Jan Antos: Software. Michal Urbanek: Methodology. Pavel Urbanek: Assisted with spectroscopic analysis, Jakub Sevcik: Assisted with spectroscopic analysis. Ivo Kuritka: Supervision, Writing – Review & Editing.

1. Introduction

The polymer thin films are affected by macromolecular chain properties, which are, at the same time, influenced by the restricted film spatial arrangement. In contrast with polymer bulk, the final thin polymer film properties do not depend only on polymer type and ambient conditions (temperature and pressure), but also on the thickness (h) and a presence of substrate (spatial restriction) and they can differ radically from the properties of the bulk [1]. If we consider temperature-dependent changes of polymer properties pronounced considerably at the temperature domain of a glass transition [2,3], a description of the system free volume (V_{free}) and relaxation time (τ) also becomes the crucial issue.

Since polymer thin films have already found their application e.g. in electronics as organic thin film transistors [4–6], or bio/medical area as various coatings [7,8], they have become an abundantly studied topic. Differences in the thermal behavior of polymer thin films contrary to bulk were reported already in the 1960s [9]. The whole temperature range of glass transition is represented with glass transition temperature (T_g) that is commonly extracted as a temperature at inflection point of the step change at DSC curve. However, it also depends on the heating rate used for polymer evaluation. The higher the heating rate the more pronounced effects at glass transition domain and shift of the T_g is observed. T_g of the polymer is influenced by macromolecular chain properties, such as chain length (M_w), engagement of intermolecular interactions, chain toughness and flexibility. In addition, the T_g of polymer thin films is not unambiguously described only with properties of polymer itself. However, the close vicinity of the macromolecules – substrate of the film, free surface of the film, multi-layered film – has to

* Corresponding author.
E-mail address: capkova@utb.cz (T. Capkova).

https://doi.org/10.1016/j.polymertesting.2021.107305
Received 1 April 2021; Received in revised form 28 June 2021; Accepted 25 July 2021
Available online 26 July 2021

be taken into consideration. The determination of thin film glass transition is thus not as routine as determination of bulk T_g by DSC, DMA or other methods, but it involves temperature resolved spectroscopy methods (dielectric spectroscopy, ellipsometry, fluorescence) [10,11] or ultrafast DSC and modulated DSC [12,13].

The decrease of T_g of the thin film below bulk T_g has been reported and can be explained by the presence of a high-mobility layer near the free surface (polymer-air interface) with lower τ [14,15], which reaches a maximum near the T_g [16]. Thin film dynamics description also involves an assumption of cooperative motions within cooperative volume or existence and competition of both high-mobility and cooperative motion region [17,18]. Glass transition is considered as a wide temperature domain with sub-domains describing particular steps of relaxation related to specific parts of macromolecules. The release of chain segments within cooperative volume is usually connected with α-transition represented with T_α (close or above T_g) [19]. However, localized motions of shorter molecular segments (i.e. side chains and groups) describing β-transition of the system are achieved at significantly lower temperatures (T_β) than T_α. Transition γ precedes both these relaxation steps, occurs at even lower temperature range than T_β and originates in the non-cooperative intramolecular dipole movement (stretching and bending of groups) [20]. Monitoring of sub-T_g transitions is convenient for full description of thermally induced molecular fluctuations and commonly conducted via dielectric spectroscopy [21] or broadband dielectric spectroscopy [22,23] analyses. The extent of cooperativity is highly influenced by the structure and size of the systems and is not as unequivocal, e.g. oligomers can provide cooperative nano-domains due to intermolecular interactions of side chains while the main chain can act as domain of non-cooperative motion [24].

Glass transition is generally (including sub-T_g transitions) connected with a release of particular molecular motions at a specific temperature range with simultaneous increase of free volume to the level needed for sub-T_g transition or liquid state formation. For a description of the temperature-dependent behavior of polymer thin films it is convenient to consider the V_{free} as a result of free vibrational volume ($V_{free:vib}$) and free excess volume ($V_{free:exs}$) as discussed in an extensive review in Ref. [25]. $V_{free:vib}$ is a genuine contribution to V_{free} of the thin film that is always present even if 3D spatial restrictions are regarded.

The influence of the film thickness on the T_g of film is another intensively discussed research topic. A reduction of T_g with decreasing thickness of the films observable usually for thicknesses below 100 nm has been reported for both free-standing films, e.g. PS [26,27] and poly (α-methyl styrene) [28] and substrate supported thin films without strong polymer-substrate interactions [29]. Glass transition thickness dependence is very often regarded as one of the fundamental characteristics of thin films. The film thickness influences a size of the cooperatively rearranging region and thus directly affects transition temperature and pronounced when thickness change from micrometer to nanometer scales [19]. Furthermore, glass transition is also influenced by polymer chain conformational (non)equilibrium and internal stresses, which originate in a film preparation procedure, such as spin coating, and involve a thermal history of the bulk polymer as well. As presumed in [30], non-annealed films could therefore manifest no T_g thickness dependence or in other words, the thickness dependence may be overlaid by other more pronounced effects.

The polymer thin films are advantageously investigated with infrared reflection-absorption (IRRAS) method or polarization-modulated IRRAS (PM-IRRAS) [31]. Determination of T_g (also indicating T_α and T_β) from PM-IRRAS spectra e.g. PS, PET and PMMA can be realized via several ways: i) a shift of absorption band and the logarithm of absorbance ratio at lower and higher energy state of given IR band plotted versus temperature which reflects mutual transformation between absorption energy state of given functional groups [32]; ii) the absorbance ratio corresponding to *trans* and *gauche* conformation (e.g. PET) plotted against temperature [33]; iii) the integrated absorbance and ratio of band areas at region 1300–1100 cm^{-1} displayed versus temperature for PMMA [34]; iv) logarithm of positive or negative absorbance plotted versus reciprocal temperature, where positive or negative absorbance is obtained from the subtracted spectra measured at a higher temperature and room temperature with the resulted determination of carbonyl fraction bonded to substrate causing substantial confinement of isotactic PMMA in comparison with syndiotactic and atactic PMMA [35]. Glass transition temperature region is then detected as a turning point at the described temperature dependencies indicated as an intersection of linear fits below and above glass transition domain. Conformational energy of the transition from *trans/gauche* conformation is possible to calculate with Van't Hoff equation [33,35]. Moreover, principal component analysis of temperature resolved PM-IRRAS spectra [36] or its combination with a 2D mapping of the first derivative of absorbance in respect to temperature [37,38] is another way of determination of T_g region.

On the contrary to fluorescence spectroscopy [27,39–42], ellipsometry [28,43,44], or x-ray reflectivity [29], a low amount of studies has been dedicated to temperature-resolved PM-IRRAS study of PS thin films, although it could help to understand the specific temperature-dependent response of individual vibrations of this polymer and bring a new insight in the revelation of sub-T_g transitions otherwise analyzed with e.g. ultrafast DSC or dielectric spectroscopy. This assumption is based on the fact that molecular response on temperature increase in IR spectra does involve alterations in the vicinity of vibrating functional groups (such as aromatic and aliphatic origin of groups, non-bonding interactions, the distance of functional groups), which reflect in $V_{free:vib}$ change and consequently describe particular contributions to glass transition.

In our study, we therefore focus on the determination of temperature influence on high-molecular-weight PS thin films from PM-IRRAS spectra and particularly from spectral region areas. We have aimed to cover the vibrational state changes considering region area and not only the absorbance or wavenumber band shifts because the precise investigation of small band shifts requires very high spectral resolution that prolongs the collection time of the spectrum, and thus, limits the heating rate (which is an important factor for investigation of glass transition) of the thin film under study. The development of region area with temperature was observed and further glass transition of thin films was described. We have verified that vibrational motions of thin polymer films cope with repeated temperature increase by two ways, without changed response to repeated heating/with changed response to repeated heating (further in the text reversibly/irreversibly), following thus the thermal and processing history of the material. A temperature-dependent abrupt change in vibrational intensity of aromatic C_{ar}-H stretching in contrary to a step-change of the intensity of C_{ar}-H out-of-plane bending and together with linear temperature response of both aliphatic C–H stretching and bending vibrations have proven that $V_{free:vib}$ is a crucial factor, which can be indirectly monitored this way. The present paper provides the new data on PS thin films obtained with PM-IRRAS and suggest a connection between PM-IRRAS results and the temperature-processing state of the thin film. Therefore, a temperature history of the polymer thin film can be revealed by this spectroscopic analysis.

2. Material and methods

2.1. Materials and thin film preparation

High-molecular-weight polystyrene (PS350; $M_w \sim 350\,000$, $M_n \sim 170\,000$) purchased from Sigma Aldrich was used as a material of thin films. Three solutions were prepared by PS350 dissolution in; 1)chloroform (TCM, grade HPLC) from J. T. Baker, 2) toluene (p.a., 99.5%) from Sigma Aldrich and 3) 1:1 mixture of both toluene and TCM (designated as Mix). PS350 was stirred with solvent at 50 °C until full dissolution to obtain clear solutions, which were used for thin film preparation. Concentration of all PS350 solutions was 30 mg/mL and 5

mg/mL. Concentrations and solvents were chosen to reach the various values of film thicknesses.

Thin films were deposited from prepared solutions on silicon (Si) and gold (Au) substrates to enable further infrared spectroscopy, thickness and surface structure analyses. The size of the substrate was 2 × 2.5 cm. Thin films were spin-coated by the static method with spin coater Laurell WS-650-MZ-23NPP with spin rate 1000 rpm with acceleration 500 rpm/min. After deposition, the films were dried at 30 °C in a vacuum oven under pressure 0.1 mbar for approx. 18 h to assure full solvent evaporation. Solvent evaporation was confirmed with a spectroscopic method (PM-IRRAS) used in this experiment. Infrared spectra of freshly prepared films (after 18 h of solvent evaporation in a vacuum) measured at room temperature were compared with spectra collected after the first heating of thin films (as described in section 2.3). No difference between these spectra and further no spectral bands indicating a presence or evaporation of solvents during heating were found.

Two series of films were prepared. First, films (films thickness; h = 19–548 nm), which were analyzed as prepared without any previous annealing to enable a study on how PS350 molecules react on the temperature increase when no relaxation of chain segments was employed. Second, films (h = 365–548 nm), which had been annealed for 4 days above PS350 bulk T_g at 130 °C to compare results with non-annealed films and demonstrate how the temperature/processing state of the film can be monitored.

2.2. Film thickness and surface structure

The thickness of thin films was measured with mechanical profilometer Dektak XT-E (Bruker, USA) with 1 nm resolution. The thickness measurement was set up with a tip radius of 2.5 μm, length of analyzed region 200 μm and stylus force 3 mg. The thickness was calculated as the average value of the three measurements. The thickness analysis was performed with films deposited on Si substrate to avoid deterioration of films prepared on the Au substrate.

The images of thin films surface deposited on Au substrates were recorded using the same instrument with a digital camera with magnification 100x. The images were taken twice. First, right after film deposition without annealing or other film treatment and then after measurement of infrared spectra, which involved sample heating (see next chapter).

2.3. Polarization-modulation infrared reflection-absorption spectroscopy

Thin films on Au substrates were analyzed with Nicolet iN10/iZ10 spectrometer (Thermo Scientific, USA) with a heated chamber Refractor-Reactor (Harrick, USA) with wedged ZnSe windows enabling grazing angle reflection-absorption measurement (incident angle 75°). The thin films on Au substrates were inserted in the chamber on a heated stage and analyzed at an increased temperature in the air atmosphere.

The measurement was performed in the mid-infrared region (MIR) in the range 4000–650 cm^{-1}. Spectra were acquired after 16 scans with a resolution 4 cm^{-1}. The wire grid polarizer on KRS-5 substrate was set to the optimal angle of 90° providing p-polarized radiation. The temperature of a heated stage and the thin film was controlled by the software EZ-ZONE® Configurator (Watlow, USA). The temperature profile was set to heating from RT to 142 °C with a rate of 2.6 °C/min. The chosen heating rate corresponds to the measurement of one spectrum per 1 °C of heating with a given resolution and number of scans. This setting enables measurement of one spectrum with minimal influence of sample heating during a particular spectrum collection and at the same time, the dynamic measurement suitable for glass transition analysis can be done. Spectra were measured in mode “one after another”, which enabled us to gain approx. 100 spectra for one thin film per one heating. Each thin film (non-annealed and annealed) was analyzed twice to observe spectral changes occurring during the first and second heating.

2.4. Differential scanning calorimetry

The differential scanning calorimetry (DSC) measurement of bulk PS was done using the LabSys Evo DTA/DSC (Setaram) instrument with TG/DSC sensor. The measurement was performed in the air atmosphere. A sample was heated from 30 °C to 170 °C with a rate of 10 °C/min and air flow 60 ml/min. The value of bulk T_g was used for comparison with transition temperatures of thin films.

3. Result and discussion

3.1. Thickness and surface structure of polystyrene thin films

Thicknesses of PS350 thin films prepared from different concentrations and solvents were determined from three locations on the sample. The individual average values with standard deviation (SD) are summarized in Table 1. To avoid any uncertainty connected with determination of sample thickness Si substrate, the thickness of the thin films on Au substrates, which were used for spectroscopic study, was also examined after the PM-IRRAS experiment. The thickness was double-checked and confirmed without the need of broad statistical analysis. All thicknesses of films obtained on Si and Au substrates were in good agreement.

With the decreasing concentration of PS350 solution, the thickness of the thin films rapidly decreases. The thickness of the film is also affected by the type of solvent and their boiling points leading to different evaporation times. The thinnest and smoothest layers with the lowest SD were prepared from a solution of PS350 in toluene. The films spin-coated from TCM were uneven which was observable especially for high-concentrated solutions. SD reached 39 nm with 30 mg/mL TCM solution, which indicates substantial surface inhomogeneity. Films deposited from solvent Mix resulted in thickness between values obtained for films prepared from individual solvents. Their SD is 2 nm and 8 nm for films from 5 mg/mL and 30 mg/mL solutions, respectively, which reveals the films are almost as homogeneous as the ones prepared from toluene solvent.

The surface structure of prepared films was observed with magnification 100x. Fig. 1 represents images of films that were taken immediately after film preparation without any additional surface treatment. As can be seen in the figure, the surface is smoothest for films spin-coated from toluene solutions (Fig. 1A and B). Similar images were taken for films prepared from Mix solution (Fig. 1C and D). Higher inhomogeneities are observable for thicker film 430 nm, while films prepared from a lower concentration have been found smoother.

Further, surface images of films prepared from TCM solution, which were taken before and after PM-IRRAS measurement are given in Fig. 2. We chose these films as representative samples, where the surface deterioration after two-fold heating from RT to 142 °C is demonstrated. The images A and C were taken after film preparation and they are compared with B and D taken after the heating procedure. New surface disruptions are present. Films (548 nm and 40 nm) contain disruptions radially oriented on the surface. Moreover, the same films exposed to heating evince holes, not only surface inhomogeneities (highlighted with the red color circles in Fig. 2). Since thin films were heated above T_g of the PS350, the effect of dewetting can also contribute to the creation

Table 1
Average thicknesses with SD of prepared thin films with different PS350 solutions.

Film deposition conditions	PS350 30 mg/mL			PS350 5 mg/mL		
	1000 rpm			1000 rpm		
	Toluene	TCM	Mix	Toluene	TCM	Mix
Thickness [nm]	365 ± 5	548 ± 39	430 ± 8	19 ± 2	40 ± 3	30 ± 2

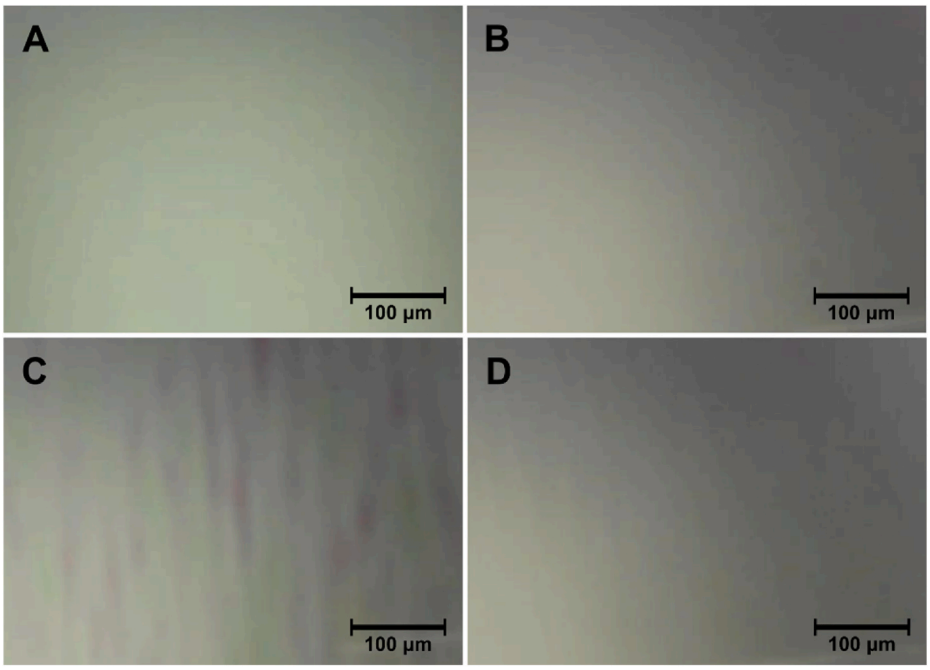

Fig. 1. The images of PS350 thin films surfaces deposited from toluene (A, B) and Mix solution (C, D) taken immediately after deposition; film thickness 365 nm (A), 19 nm (B), 430 nm (C) and 30 nm (D). Zoom 100x.

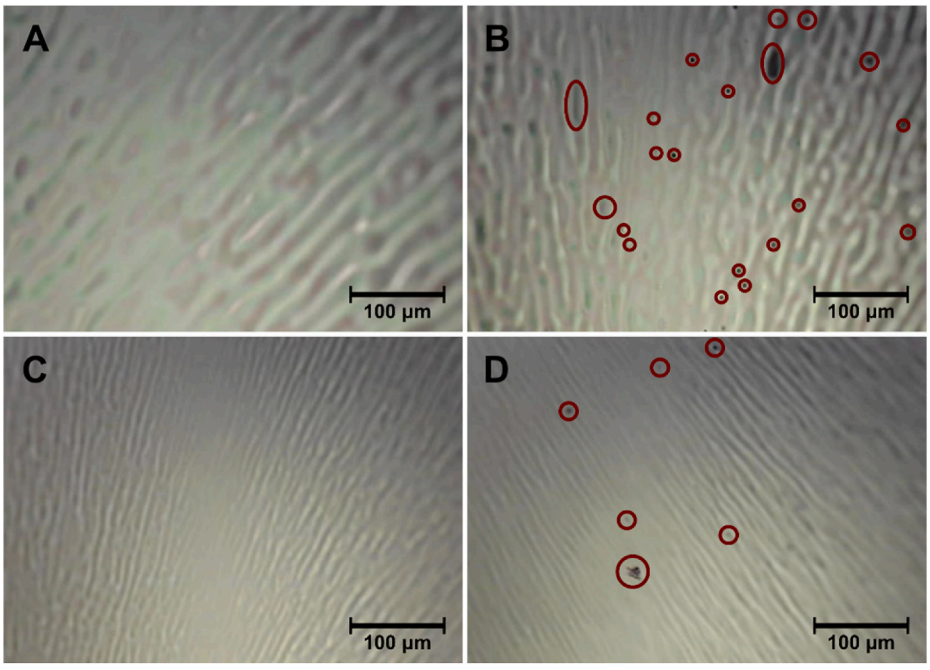

Fig. 2. The images of PS350 thin film surfaces deposited from TCM solution before PM-IRRAS measurement (A, C) of film 548 nm and 40 nm, respectively and after two-fold heating of PM-IRRAS measurement (B, D) of film 548 nm and 40 nm, respectively. Zoom 100x.

of holes on the surface. It has been shown that thin films of PS on the sputtered gold surface [45] as well as on the silicon surface [46] are prone to dewet if no anti-dewetting measures [47,48], are considered. All studied PS350 films were influenced by sample heating and their surface evince disruptions, although films prepared from toluene and Mix solvent were less disrupted.

As a result, toluene with a higher boiling point is more suitable for PS350 thin film preparation. Long polymer chains have more time to arrange on the substrate surface and thus create a homogenous layer, while quicker evaporation of TCM with a lower boiling point causes immediate immobilization of polymer chains on the substrate in the radial shape after spin-coating without sufficient relaxation. This also corresponds with a thickness variance of films. The surface structure of the film can therefore be tailored with specific spin-coating conditions and the use of solvent.

3.2. PM-IRRAS regions analysis for determination of transition temperature

We have focused on the temperature (T), and thus glass transition

influence on PM-IRRAS spectra of high-molecular-weight PS350 in the form of Au-supported thin films with thickness ranging from 19 to 548 nm. IR spectrum of PS350 was divided into four regions, 3120–2985 cm^{-1}, 2980–2825 cm^{-1}, 1470–1430 cm^{-1} and 810–675 cm^{-1} (725–675 cm^{-1}), covering C_{ar}-H, C–H and C_{ar}-C_{ar} stretching and bending vibration of phenyl ring as well as of aliphatic PS350 groups, which are given in Fig. 3 together with a scheme of corresponding vibrational motions. The assignment of all PS350 vibrational bands, which are discussed in the paper, is routine and can be found in fundamental literature [49]. The upper parts of Fig. 3 show the spectra of the thinnest film with a thickness of 19 nm, while the bottom part is dedicated to the thickest film of 548 nm. Films 548 nm, 430 nm, and 365 nm had also been subjected to annealing for 4 days before PM-IRRAS measurement for comparison with non-annealed films. Only the three thickest films had been chosen for the annealing experiment because the intensity of the spectral bands of the thinnest film is ten times lower than the intensity of 548 nm film, as shown in Fig. 3. It seems that we have reached detection limits (at given experimental setup of 16 scans, resolution 4 cm^{-1} and heating rate 2.6 °C/min) with films of thickness below 100 nm, when the signal-to-noise ratio decreased significantly and spectra had not been sufficiently smooth. However, in order to follow the principle of T_g determination, a decrease of the heating rate was unacceptable. The vibrational bands in Fig. 3A and 3103 (3101), 3082 (3079), 3059 (3058), 3025 (3024) and 3000 (2999) cm^{-1}, represent aromatic C_{ar}-H stretching vibrations of phenyl ring at 30 °C and 142 °C; the shift of the band at 142 °C is shown in brackets. A clear shift of band maxima to lower wavenumbers with temperature has been observable for all films, which indicates that vibrational motions are at higher temperatures energetically less demanding. On the other hand, no significant change in band position from the first and second heating of the films was observed, which is demonstrated with overlaid spectra. Similar trends were registered in the spectral region 2980 – 2825 cm^{-1}, which belongs to the stretching vibration of C–H groups given in Fig. 3B. The spectral bands 2923 cm^{-1} and 2850 cm^{-1} do not react on increased temperature and their wavenumber position is stable. Another region of interest 1470–1430 cm^{-1} is given in Fig. 3C. The band 1452 cm^{-1} represents CH_2 bending vibrations (scissoring) from the aliphatic part of PS350 macromolecule. This band also involves C_{ar}-C_{ar} stretching vibrations of phenyl. The shift of band maxima between RT and 142 °C has been determined within 1 cm^{-1}. Fig. 3D shows region 810–675 cm^{-1} of spectral bands 758 (756) cm^{-1} and 702 (701) cm^{-1} that belong to C_{ar}-H out-of-plane bending vibrations and aromatic ring out-of-plane deformation, respectively, of the mono-substituted phenyl ring. The band 702 cm^{-1} has the highest intensity in the whole PS350 spectrum.

3.3. Temperature impact on PM-IRRAS spectra

All of the mentioned spectral regions were baseline corrected. Their area (A_i, where i is the range of spectral region) was calculated by mathematical integration of the spectrum curve and plotted against temperature. The statistically detected outliers were omitted from further evaluation.

The whole regions, not only wavenumber shift or band absorbance, were investigated in dependence on T. We suppose that the temperature response of a particular thin film spectral region can be involved in the area values, as was shown for PS pellets previously [50]. The advantage of this method is that the intensities of individual bands are also reflected in the area of the selected region without a need of spectrum deconvolution. Therefore, from the plot A_i vs. T, a turning point or step-change in the temperature region was detected. This temperature is here assigned to individual functional group transition describing the local molecular motions and β-transition of PS350 thin films.

We found that particular regions of the PM-IRRAS spectrum respond specifically to a temperature increase. This response is influenced predominantly by the heating (and processing) history of the sample, i.e. vibrational reactions were detected to be temperature specific and

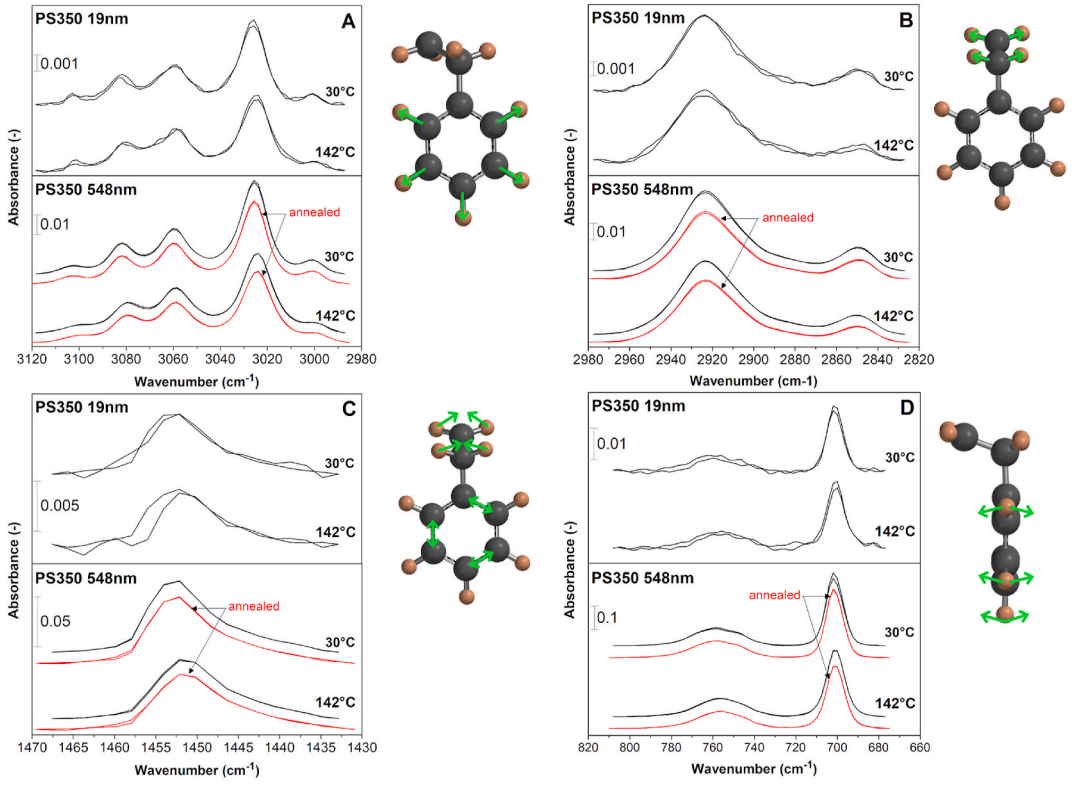

Fig. 3. Region 3120–2985 cm^{-1} (A), 2980–2825 cm^{-1} (B), 1470–1430 cm^{-1} (C) and 810–675 cm^{-1} (D) of IR spectra of thin films measured at 30 °C and 142 °C in air. Pairs of overlaid spectra of the same color represent first and second heating. PS350 vibrational motions are schematically depicted on the right of each graph. (For interpretation of the references to color in this figure legend, the reader is referred to the Web version of this article.)

moreover some of them are sensitive to repeated heating of the film. If A_i is calculated from the spectra obtained during initial sample heating from RT to 142 °C, we can observe that A_i follows clear trends. This was confirmed for non-annealed films with all studied thicknesses. These trends can be divided into three groups: (i) A turning point in A_i dependence on temperature characterized by an abrupt change of linear curve slope value can be detected. At this point, A_i usually reaches a minimum and further rises with increasing temperature. This trend is typical for the region of C_{ar}-H stretching and transition temperature is extracted at a minimum. (ii) Two turning points are present in A_i versus T plot providing a step-change of A_i value. Therefore, temperature range, where A_i values change significantly, is found. Region of C_{ar}-H out-of-plane bending is representative of this behavior, from which onset (T_{onset}) and endpoint (T_{end}) temperatures of this transition are found. (iii) A_i declines linearly in the whole temperature range (L, linear change) and thus no temperature value/region that would significantly affect and therefore alter a vibrational behavior is found. This is the case of both C–H stretching and the bending region. Regarding the monitoring of vibrational motions and their influence by vicinity of the vibrating atoms, e.g. release of the side group motions, the transition temperature or region of temperatures here detected is probably related to β-transition of the polymer in the thin film.

The heating as well as annealing of the thin films caused unique differentiation of the behavior of the spectral regions and thus vibrational motions. Regions 3120–2985 cm^{-1}, 2980–2825 cm^{-1} and 1470–1430 cm^{-1} have kept the A_i vs. T trends even after repeated heating or annealing of the films. These unchanged trends are in this text regarded as reversible. On the contrary, the spectral region of C_{ar}-H out-of-plane bending (810–675 cm^{-1}, 725–675 cm^{-1}) has undoubtedly evinced irreversible temperature response induced by repeated heating or annealing of the film because the course of A_i vs. T has differed substantially from the original trend.

Determined values of transition temperature assigned to T_β from spectra recorded in the ambient air are summarized in Table 2. T_1 and T_2 have been gained from the initial and repeated heating of thin films, respectively. In the case of stepwise temperature change, the upper and lower limit is given as a range of T_1 or T_2, however indicating T_{onset} and T_{end} of the β-transition. The values obtained for annealed films are given in brackets. IRRAS spectra of films with thickness 19–40 nm had substantially been loaded with spectral noise, which inserted higher uncertainty in the determined temperatures as can be seen in Table 2. For this reason, all figures related to the thinnest films are provided only in Supplementary data.

The following part describes spectral regions of interest from the viewpoint of sub-T_g transition, found A_i trends and chemical structure. The results are compared with bulk PS350 T_g, which was determined by DSC to be 108 °C in the air. DSC curve of PS350 is available in Supplementary data in Fig. S1.

Region of C_{ar}-H and C–H stretching

Fig. 4 represents data of calculated areas from spectral regions 3120–2985 cm^{-1}. Aromatic C_{ar}-H stretching vibrations belonging to phenyl rings of PS350 evince a slight decrease of $A_{3120\text{-}2985}$ with increasing temperature until the turning point is reached and then increases continuously. The T_1 is 81 °C (92 °C), 80 °C (98 °C), 84 °C (98 °C) for non-annealed and annealed (in brackets) films measured with thickness 548 nm, 430 nm and 356 nm, respectively. The trend of $A_{3120\text{-}2985}$ vs. T plotted from repeated heating of films has not changed and T_2 is several degrees higher than T_1, reaching 100 °C for annealed films. This behavior is thus independent of the heating history of thin film and can be explained by two opposite effects that influence the vibrational intensity. The density of thin film decreases with increasing temperature leading to a slight decline of the spectral region intensity and at the same time, the free volume of the system becomes larger with an increasing temperature that on the contrary enables the further increase of the vibrational intensity [50,51]. Each of these two effects prevails at different temperature ranges, and close to transition temperature, the area of the spectral region reaches its minimum. Below T_g, segmental motions are frozen and the vibrational intensity of in-plane C_{ar}-H stretching is almost constant and slightly decreases until the point of glass transition is reached. Nevertheless, stretching vibration is also the main contribution to molecular movement because the segments are stuck, and the temperature domain where change occur is thus rather regarded as β-transition than α-transition. At the turning-point temperature, the intensity of this vibration begins to rise because a release of the side group motions causes significant alterations in the vicinity of aromatic rings that provide stretching vibrations. This leads to the following conclusion; the β-transition of polymers in the thin film evinces the dependence on the free volume and the change in free vibrational volume caused by C_{ar}-H stretching is thus expectable and reflected in $A_{3120\text{-}2985}$ increase above T_β. Moreover, a comparable increase of polymer free volume was described from molecular dynamics simulation in Ref. [52] and our results of A_i follow the identical trend. Temperature values extracted from the plots are in the case of non-annealed films rather lower than T_g of bulk PS350, however, they reached to 100 °C after the annealing procedure of films. This agrees with the character of β-transition, whose temperature range is below T_α (T_g). The non-annealed thin film generally has an unknown processing history of polymer and a considerable amount of internal stress gained during spin-coating process that can even lead to thickness independent values of transition temperature [30]. Moreover, the annealing process depends on the M_w and relaxation time of the polymer and initial film thickness. The time and temperature of annealing have to be chosen by a compromise between the long time needed for a relaxation of chains especially with very high M_w of polymer and the temperature above T_g of the bulk, which can cause the undesirable film dewetting without sufficient relaxation. Nevertheless, we did not consider the T_β thickness dependence from region 3120–2985 cm^{-1} as all three annealed films are thicker than 100 nm and no temperature value was determined from plots of the thinnest films. $A_{3120\text{-}2985}$ vs. T for films of 40–19 nm can be found in Supplementary data – Fig. S2.

On the contrary, C–H stretching vibrations region belonging to

Table 2
T_β according to spectral regions of non-annealed (annealed) PS350 films in air.

PS350 air	3120–2985 [cm^{-1}]		2980–2825 [cm^{-1}]		1470–1430 [cm^{-1}]		810–675 [cm^{-1}]		725–675 [cm^{-1}]	
h [nm]	T_1 [°C]	T_2 [°C]	T_1 [°C]	T_2 [°C]	T_1 [°C]	T_2 [°C]	T_1 [°C]	T_2 [°C]	T_1 [°C]	T_2 [°C]
548	81 (92)	82 (95)	L (L)	L (L)	L (L)	L (L)	67-87 (—)	— (—)	65-86 (—)	— (—)
430	80 (98)	80 (100)	L (L)	L (L)	L (L)	L (L)	63-82 (—)	— (—)	60-81 (—)	— (—)
365	84 (98)	85 (97)	L (L)	L (L)	L (L)	L (L)	63-87 (—)	— (—)	62-86 (—)	— (—)
40	—	N/A	L	L	L	N/A	70–102	—	70–100	—
30	N/A	N/A	L	—	L	L	85–100	—	70–100	—
19	N/A	N/A	L	—	L	N/A	N/A	N/A	N/A	N/A

h = film thickness; T_1 and T_2 = temperature of a turning point or temperature range extracted from A_i vs. T dependence obtained from initial and repeated heating of the same film, respectively; L = linear decrease of A_i in investigated temperature range; — no change of A_i with T; N/A no clear trend, high data variation. Data for annealed films are given in brackets.

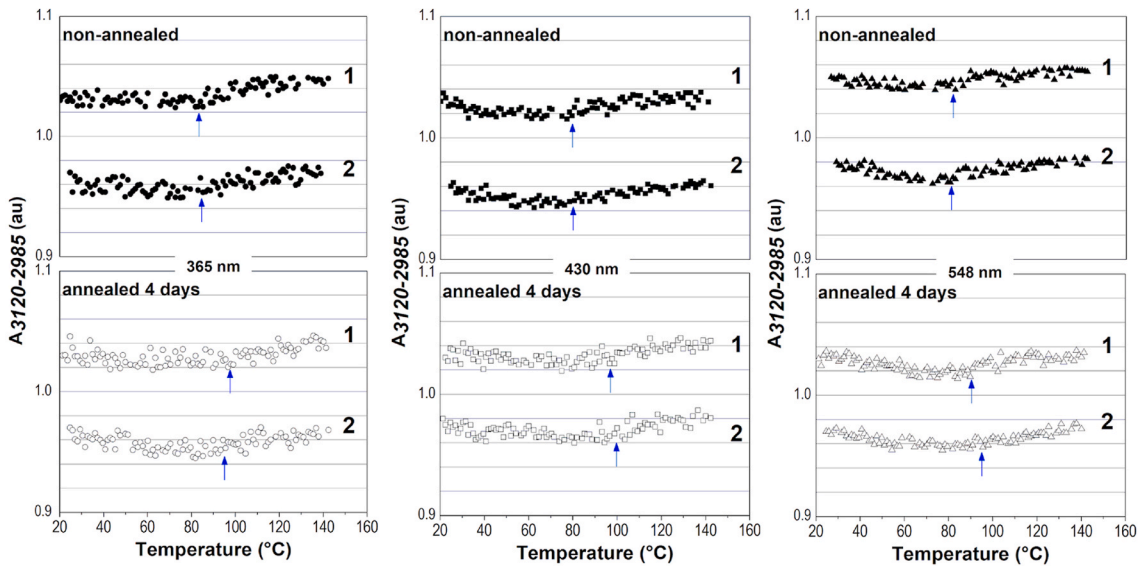

Fig. 4. $A_{3120–2985}$ plotted against temperature from the initial (1) and repeated (2) heating of non-annealed and annealed films (365–548 nm) in the air.

aliphatic PS350 groups behave differently as shown in Fig. 5. T_1 and T_2 were not detected and $A_{2980\text{-}2825}$ decreases gradually with increasing temperature. This trend was found for all films. The intensity of aliphatic C–H stretching vibrations thus drops with increasing temperature and is thickness independent for films treated during both heating procedures, as well as annealing.

This result indicates that the same vibrational type of a similar functional group (same atoms, different electron distribution) can react divergently on temperature. In the case of aliphatic C–H stretching the decrease of $A_{2980\text{-}2825}$ is led by the effect of decreasing film density, which can be joined with thin film dewetting as was reported for films thinner than end-to-end macromolecular distance [53]. C–H groups are in comparison with phenyl rings small and are located close to the PS350 backbone. Hence, their indifference to any significant temperature response can be rationalized again with the viewpoint of free volume, i. e. their vibrational motions occur always at the space close to the backbone and as a result, they are not influenced with either side groups motions, or even segmental motions to such an extent as aromatic vibrations are and they occupy the same amount of free vibrational volume regardless the temperature increase. $A_{2980\text{-}2825}$ vs. T for films of 40–19 nm are given in Supplementary data – Fig. S3.

C_{ar}-H and C–H stretching vibrational motions can therefore be distinguished with different temperature dynamics, which reflects that C_{ar}-H stretching is more susceptible to temperature change and describes T_β by reversed course of $A_{3120\text{-}2985}$ continuous decrease. While $A_{2980\text{-}2825}$ gradually decreases in the whole temperature range.

Region of CH_2 in-plane bending and C_{ar}-C_{ar} stretching

CH_2 scissoring vibrations of aliphatic groups together with C_{ar}-C_{ar} stretching of PS350 (1470–1430 cm^{-1}) were found to behave similarly to corresponding C–H stretching vibrations. As can be found in Fig. 6, $A_{1470\text{-}1430}$ decreases linearly with temperature and T_1 and T_2 were detected neither for non-annealed, nor annealed films of 365–548 nm. The same results were found for thicknesses 19–40 nm given in the Supplementary data – Fig. S4. The explanation of a continuous decrease of $A_{1470\text{-}1430}$ with T is analogous to the previous region 2980–2825 cm^{-1}. As C–H stretching, C–H scissoring vibrations occur in the small volume around the PS350 backbone, which does not bring any

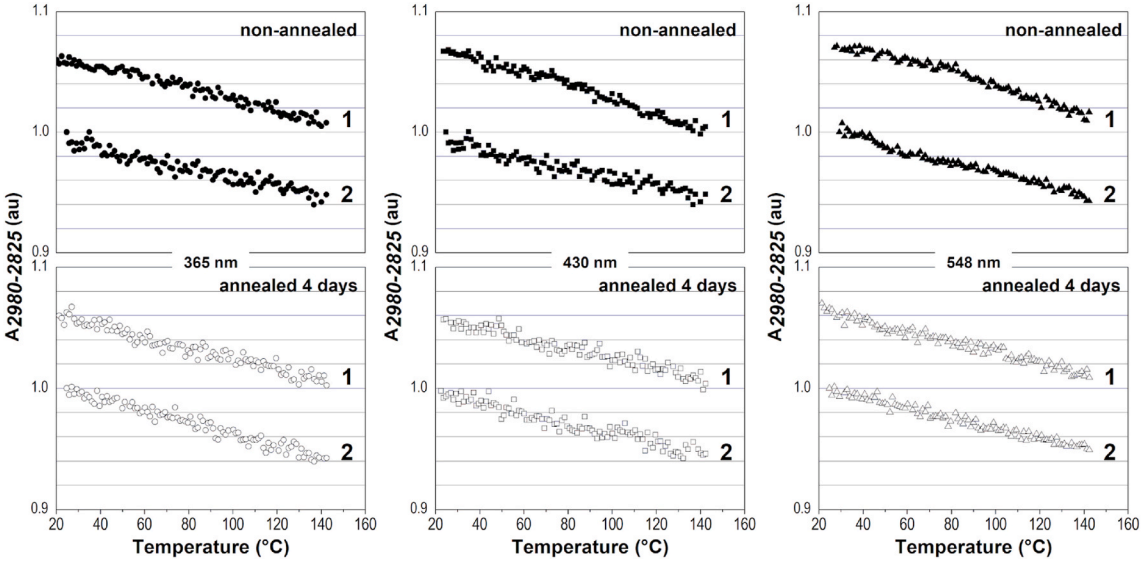

Fig. 5. $A_{2980\text{-}2825}$ plotted against temperature from the initial (1) and repeated (2) heating of non-annealed and annealed films (365–548 nm) in the air.

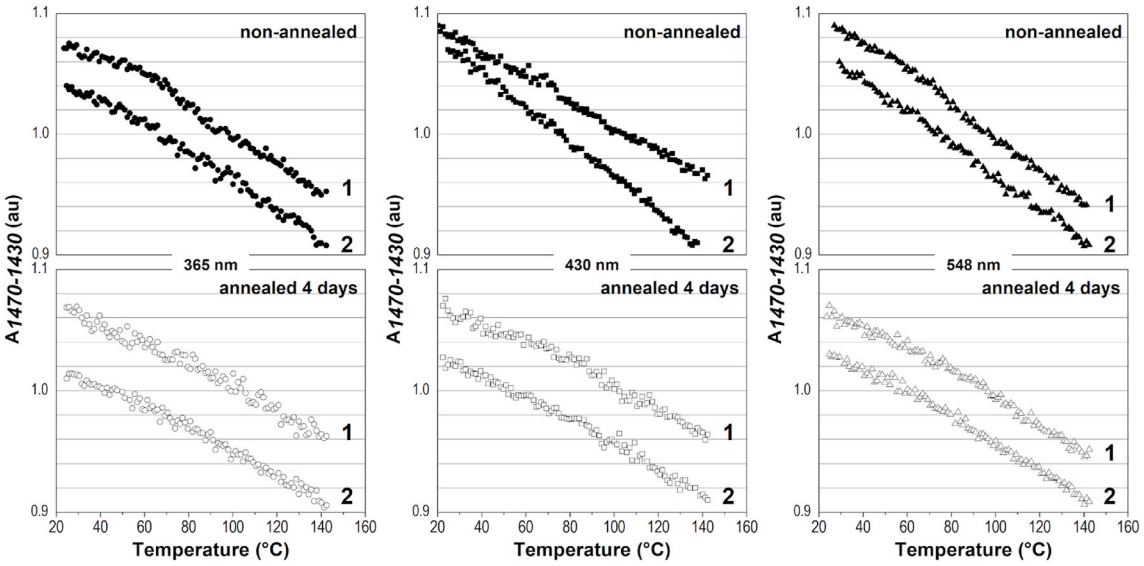

Fig. 6. $A_{1470\text{-}1430}$ plotted against temperature from the initial (1) and repeated (2) heating of non-annealed and annealed films (365–548 nm) in the air.

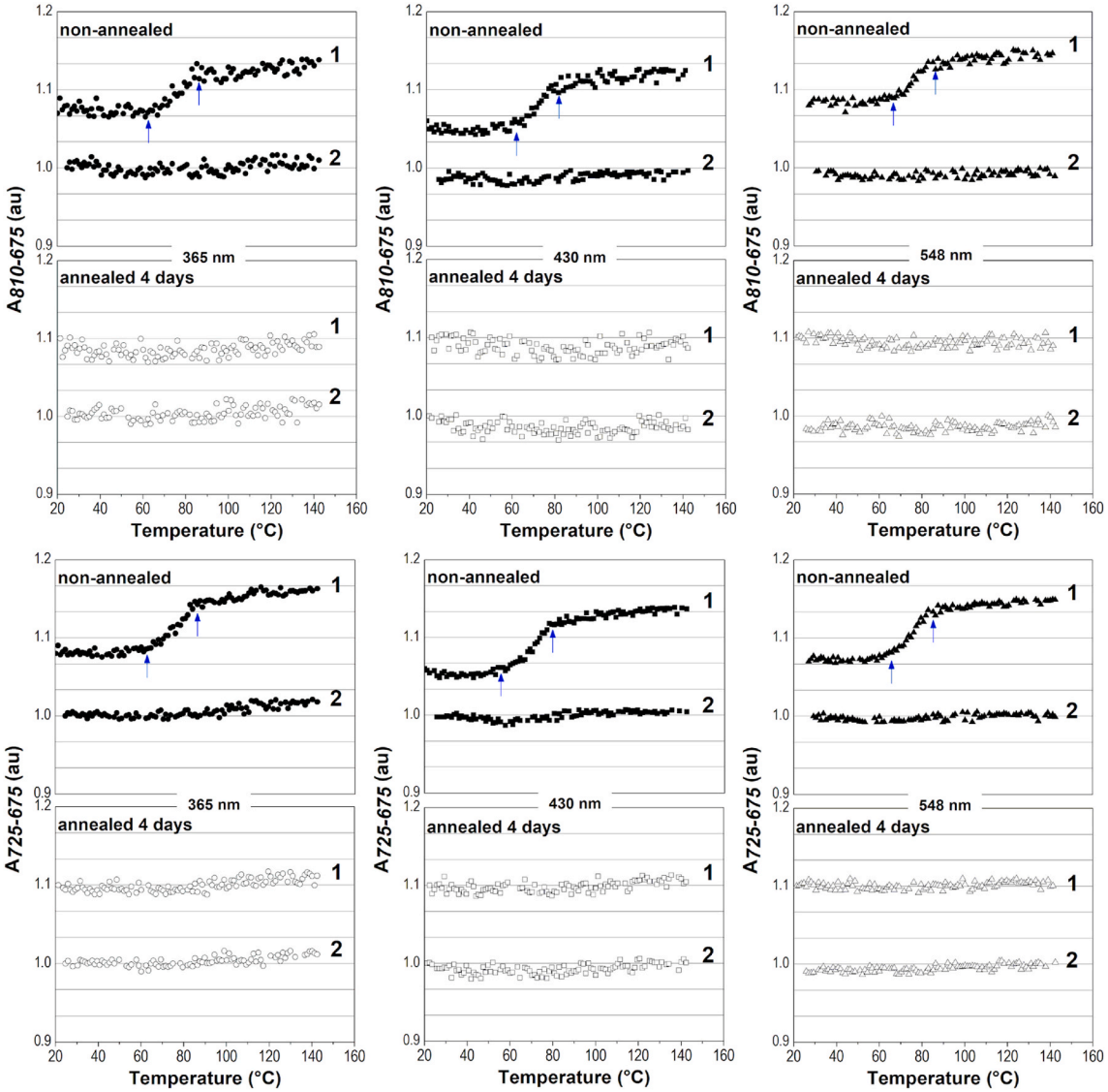

Fig. 7. $A_{810\text{-}675}$ and $A_{725\text{-}675}$ plotted against temperature from the initial (1) and repeated (2) heating of non-annealed and annealed films (365–548 nm) in the air.

significant temperature breakpoint in $A_{1470\text{-}1430}$ vs. T. C_{ar}-C_{ar} stretching also contributes to this spectral region. Nevertheless, it is acceptable that it does not cause a significant deviation of the decreasing trend as this vibration manifests motions in-plane of the phenyl ring. If compared with $A_{2980\text{-}2825}$, the decrease of $A_{1470\text{-}1430}$ is steeper.

All these three spectral regions have not changed the main course of A_i vs. T with repeated heating or annealing of thin films, so that their temperature response is reversible. This indicates that they are not sensitive to temperature history.

C_{ar}-H out-of-plane bending

Another region of interest is 810–675 cm^{-1} of C_{ar}-H out-of-plane bending of PS350 and it has provided important results. These vibrational bands in IR spectra are used for the identification of aromatic ring substitution and provide essential information about the structure. A course of $A_{810\text{-}675}$ and $A_{725\text{-}675}$ vs. T is displayed in Fig. 7. It was discovered that there is no one turning point temperature, which causes the abrupt change of slope in A_i vs. T. Instead, the temperature ranges 67–87 °C (—), 63–82 °C (—), 63–87 °C (—) for non-annealed (annealed) films, in which $A_{810\text{-}675}$ increases step-wisely, had been detected only during initial heating of non-annealed films of 548, 430 and 365 nm thickness, respectively. The response of C_{ar}-H out-of-plane bending to temperature is thus considered to be irreversible, i.e. no T_β or range of temperatures limited with T_{onset} and T_{end} has been detected from both the PM-IRRAS with second heating of non-annealed films and the initial PM-IRRAS analysis of annealed films. The value of $A_{810\text{-}675}$ becomes roughly constant when the thin film is analyzed after any previous heating. This supported the strict dependence on the temperature history of region 810–675 cm^{-1}. Thinner films (40–19 nm), depicted in Supplementary data – Fig. S5, evince the same irreversible behavior with rare deviations from the step change of A_i caused predominantly by higher noise in the spectral data. The same temperature dependence was reported also for other thin film analysis – ellipsometry; it was found that the glass transition temperature region becomes broader with decreasing film thickness [43], which is in agreement with our results obtained from a different spectroscopic method. Thus, C_{ar}-H out-of-plane bending reflects the whole β-transition from the beginning with T_{onset} to the end with T_{end}. This vibrational intensity change is the most pronounced from all studied regions. Macromolecular chains are arranged randomly in the amorphous glassy state, however, phenyl rings occupy a substantial amount of the macromolecular chain volume and also protrude from the backbone. Their vibrational motions and especially out-of-plane vibrations are influenced with mutual non-bonding interactions of aromatic rings, which certainly reflects in free vibrational volume and its increase with temperature. The temperature region involving β-transition takes 20 °C for films of 548 nm, 19 °C for 430 nm, while it broadens to 24 °C for 365 nm.

A zoomed region 725–675 cm^{-1} of phenyl ring out-of-plane deformation was also evaluated with almost identical results. As can be seen in Fig. 7 and Supplementary data – Fig. S6, the data variation is lower for this region, providing thus more precise results and clearer trends. When $A_{720\text{-}675}$ from initial heating of non-annealed films was plotted against T, step-like $A_{725\text{-}675}$ increase was found and confirmed obtained values of T_{onset} and T_{end} (65–86 °C, 60–81 °C, 62–86 °C).

At this point, we would like to discuss a similarity of the results obtained from a single PM-IRRAS measurement with experimental findings provided by temperature-modulated FTIR (TMFTIR), even though they are based on a different principle. In TMFTIR, spectral bands that characterize structural changes of a sample, such as conformational change or crystallization, are observed. An irreversible and reversible intensity of the regarded vibrational band represents a kinetic and thermodynamic term, respectively, which together form the total intensity of the vibrational band [54–56]. As was shown for PET in [54], middle point T_g is determined from reversing part of total IR intensity as a change in slope curve. This is in very good agreement with our results obtained from region 3120–2985 cm^{-1} of C_{ar}-H stretching. Even though, the temperature modulation has not been used in the present experiment and therefore the total intensity of the region has been considered, its reversibility was confirmed by a repetition of the PM-IRRAS analysis on the same thin film. On the other hand, step-like change of C_{ar}-H out-of-plane bending was found to be an irreversible manifestation of various relaxations of frozen strains accompanying the sub-T_g transition. This can be again compared to the irreversible intensity from TMFTIR. If it is considered as a kinetic contribution of the total intensity, the released movement of phenyl rings that sustain non-bonding interactions does increase the vibrational intensity. However, after re-cooling of the film, phenyl rings freeze in different random positions with different extent of non-bonding interactions and therefore repeated heating does not induce exactly the same temperature response. Restricted space of thin film must be kept in mind as well as macromolecular chain constraints, which might encourage temperature irreversibility of this vibrational motion. Regarding the temperature ranges, approx. 60–85 °C, that were obtained for non-annealed films from our experiment for region 810–675 cm^{-1} and corresponding temperature value of 80 °C determined from C_{ar}-H stretching region after initial heating of the same non-annealed films, it is probable that C_{ar}-H out-of-plane bending vibrations actually provide T_{onset} and T_{end} of β-transition rather than characterization of the actual glass transition.

4. Conclusions

The paper deals with the influence of temperature on vibrational motions of Au-supported thin films made of high-molecular-weight polystyrene PS350. No interaction with Au substrate was expected and films were analyzed in two sets, non-annealed and annealed at 130 °C for 4 days. From the PM-IRRAS spectra, the area of spectral region A_i was calculated and plotted against temperature. According to obtained results, the individual vibrational motions of thin PS350 films respond uniquely to the increasing temperature describing thus sub-T_g transitions of a local effect on a macromolecular chain. While C_{ar}-H stretching vibrations reflect the increasing temperature with an abrupt alteration of the area of their spectral region and provide middle-point temperature of β-transition, C_{ar}-H out-of-plane bending vibrations increase their intensity in the step that covers a temperature range that extents below and above T_β, providing edge-point temperatures of transition, T_{onset} and T_{end}. On the other hand, aliphatic C–H stretching and bending seem to be resistant to temperature changes and their response is represented with continuous intensity decrease. This can be explained by the fact that C_{ar}-H vibrations are highly influenced by intra/inter-molecular interactions of phenyl rings, including π-π interactions. Moreover, C_{ar}-H stretching is performed in the plane of the aromatic ring, while C_{ar}-H out-of-plane bending reaches above and below the aromatic ring plane and this vibration is thus more sensitive to the interaction of phenyl rings as it occupies more free volume in the vicinity of the ring. As the macromolecular chains begin their side groups motions the C_{ar}-H out-of-plane bending is influenced immediately corresponding to T_{onset} and undergoes a transition up to T_{end}, while the C_{ar}-H stretching conducted in plane of the ring does not indicate any significant change in vibrational intensity until the middle (inflection) point of transition is reached, and then change occurs at once. A course of A_i vs. T can be considered as reversible (if no change of the main course occurs after repeated heating or annealing) or irreversible (if the significant change of the main course occurs after repeated heating or annealing). Now, it is demonstrated for PS that it should be possible to obtain temperature range of β-transition by single PM-IRRAS experiment with linear heating rate and estimate the temperature history of the thin film. If an unknown PS film is going to be investigated, it should be possible to reveal whether it has been heated above T_g ever before according to region 810–675 cm^{-1} or 725–675 cm^{-1} and their area dependences on the temperature.

CRediT authorship contribution statement

Barbora Hanulikova: Conceptualization, Formal analysis, Data curation, Writing – Original Draft. **Tereza Capkova:** Investigation, Validation, Data curation, Writing – Original Draft. **Jan Antos:** Software. **Michal Urbanek:** Methodology. **Pavel Urbanek:** Assisted with spectroscopic analysis, **Jakub Sevcik:** Assisted with spectroscopic analysis. **Ivo Kuritka:** Supervision, Writing – Review & Editing.

Declaration of competing interest

The authors declare that they have no known competing financial interests or personal relationships that could have appeared to influence the work reported in this paper.

Acknowledgment

The work was supported by the grant from the Czech Science Foundation (Project No. 19-23513S). This work was also supported by Operational Program Research and Development for Innovations cofounded by the European Regional Development Fund (ERDF) and national budget of the Czech Republic, within the framework of the project CPS - strengthening research capacity (reg. number: CZ.1.05/2.1.00/19.0409). Authors T.C. and J.A. are especially thankful to the Ministry of Education, Youth and Sports of the Czech Republic – DKRVO (RP/CPS/2020/006).

Appendix A. Supplementary data

Supplementary data to this article can be found online at https://doi.org/10.1016/j.polymertesting.2021.107305.

References

[1] R.P. White, J.E.G. Lipson, To understand film dynamics look to the bulk, Phys. Rev. Lett. 125 (5) (2020), 058002, https://doi.org/10.1103/PhysRevLett.125.058002.
[2] I.M. Kalogeras, H.E. Hagg Lobland, The nature of the glassy state: structure and glass transitions, J. Mater. Educ. 34 (3) (2012) 69.
[3] W. Brostow, H.E.H. Lobland, Materials: Introduction and Applications, John Wiley & Sons, 2017.
[4] L. Chou, Y. Na, C. Park, M.S. Park, I. Osaka, F.S. Kim, C. Liu, Semiconducting small molecule/polymer blends for organic transistors, Polymer 191 (2020) 122208, https://doi.org/10.1016/j.polymer.2020.122208.
[5] M. Pandey, N. Kumari, S. Nagamatsu, S.S. Pandey, Recent advances in the orientation of conjugated polymers for organic field-effect transistors, J. Mater. Chem. C. 7 (43) (2019) 13323–13351, https://doi.org/10.1039/c9tc04397g.
[6] S. Riera-Galindo, F. Leonardi, R. Pfattner, M. Mas-Torrent, Organic semiconductor/polymer blend films for organic field-effect transistors, Adv. Mater. Technol. 4 (9) (2019) 1900104, https://doi.org/10.1002/admt.201900104.
[7] T. Zada, M. Reches, D. Mandler, Antifouling and antimicrobial coatings based on sol-gel films, J. Sol. Gel Sci. Technol.l. 95 (2020) 609–619, https://doi.org/10.1007/s10971-020-05324-w.
[8] M. Golda-Cepa, K. Engvall, M. Hakkarainen, A. Kotarba, Recent progress on parylene C polymer for biomedical applications: a review, Prog. Org. Coating 140 (2020) 105493, https://doi.org/10.1016/j.porgcoat.2019.105493.
[9] A. Anton, Detection of polymer transition temperatures by infrared absorption spectrometry, J. Appl. Polym. Sci. 12 (9) (1968) 2117, https://doi.org/10.1002/app.1968.070120915. &.
[10] M. Erber, A. Khalyavina, K.- Eichhorn, B.I. Voit, Variations in the glass transition temperature of polyester with special architectures confined in thin films, Polymer 51 (1) (2010) 129–135, https://doi.org/10.1016/j.polymer.2009.11.032.
[11] M. Erber, M. Tress, E.U. Mapesa, A. Serghei, K. Eichhorn, B. Voit, F. Kremer, Glassy dynamics and glass transition in thin polymer layers of PMMA deposited on different substrates, Macromolecules 43 (18) (2010) 7729–7733, https://doi.org/10.1021/ma100912r.
[12] K. Schroeter, Glass transition of heterogeneous polymeric systems studied by calorimetry, J. Therm. Anal. Calorim. 98 (3) (2009) 591–599, https://doi.org/10.1007/s10973-009-0269-z.
[13] S. Gao, Y.P. Koh, S.L. Simon, Calorimetric glass transition of single polystyrene ultrathin films, Macromolecules 46 (2) (2013) 562–570, https://doi.org/10.1021/ma3020036.
[14] J.L. Keddie, R. Jones, R.A. Cory, Size-dependent depression of the glass-transition temperature in polymer-films, Europhys. Lett. 27 (1) (1994) 59–64, https://doi.org/10.1209/0295-5075/27/1/011.
[15] P.Z. Hanakata, J.F. Douglas, F.W. Starr, Interfacial mobility scale determines the scale of collective motion and relaxation rate in polymer films, Nat. Commun. 5 (2014) 4163, https://doi.org/10.1038/ncomms5163.
[16] W. Zhang, F.W. Starr, J.F. Douglas, Reconciling computational and experimental trends in the temperature dependence of the interfacial mobility of polymer films, J. Chem. Phys. 152 (12) (2020) 124703, https://doi.org/10.1063/1.5144262.
[17] J.A. Forrest, J. Mattsson, Reductions of the glass transition temperature in thin polymer films: probing the length scale of cooperative dynamics, Phys. Rev. E 61 (1) (2000) R53–R56, https://doi.org/10.1103/PhysRevE.61.R53.
[18] R.J. Lang, D.S. Simmons, Interfacial dynamic length scales in the glass transition of a model freestanding polymer film and their connection to cooperative motion, Macromolecules 46 (24) (2013) 9818–9825, https://doi.org/10.1021/ma401525q.
[19] K. Arabeche, L. Delbreilh, R. Adhikari, G.H. Michler, A. Hiltner, E. Baer, J. Saiter, Study of the cooperativity at the glass transition temperature in PC/PMMA multilayered films: influence of thickness reduction from macro- to nanoscale, Polymer 53 (6) (2012) 1355–1361, https://doi.org/10.1016/j.polymer.2012.01.045.
[20] J.D. Badia, R. Teruel-Juanes, C. Acebo, O. Gil-Castell, A. Serra, A. Ribes-Greus, Dielectric spectroscopy of novel thiol-ene/epoxy thermosets obtained from allyl-modified hyperbranched poly(ethyleneimine) and diglycidylether of bisphenol A, Eur. Polym. J. 113 (2019) 98–106, https://doi.org/10.1016/j.eurpolymj.2019.01.001.
[21] M. Soccio, A. Nogales, T.A. Ezquerra, N. Lotti, A. Munari, Effect of copolymerization in the dynamics of poly(trimethylene terephthalate), Macromolecules 45 (1) (2012) 180–188, https://doi.org/10.1021/ma202361r.
[22] I. Irska, A. Linares, E. Piesowicz, S. Paszkiewicz, Z. Roslaniec, A. Nogales, T. A. Ezquerra, Dielectric spectroscopy of novel bio-based aliphatic-aromatic block copolymers: poly(butylene terephthalate)-b-poly(lactic acid), Eur. Phys. J. E. 42 (8) (2019) 107, https://doi.org/10.1140/epje/i2019-11874-y.
[23] P. Lunkenheimer, A. Loidl, Glassy Dynamics: from Millihertz to Terahertz, Scaling of Relaxation Processes, 2018, pp. 23–59, https://doi.org/10.1007/978-3-319-72706-6_2.
[24] A. Dhotel, Z. Chen, J. Sun, B. Youssef, J. Saiter, A. Schoenhals, L. Tan, L. Delbreilh, From monomers to self-assembled monolayers: the evolution of molecular mobility with structural confinements, Soft Matter 11 (4) (2015) 719–731, https://doi.org/10.1039/c4sm01893a.
[25] R.P. White, J.E.G. Lipson, Polymer free volume and its connection to the glass transition, Macromolecules 49 (11) (2016) 3987–4007, https://doi.org/10.1021/acs.macromol.6b00215.
[26] J.A. Forrest, K. DalnokiVeress, J.R. Stevens, J.R. Dutcher, Effect of free surfaces on the glass transition temperature of thin polymer films (vol 77, pg 2002, Phys. Rev. Lett. 77 (19) (1996) 4108, https://doi.org/10.1103/PhysRevLett.77.4108, 1996.
[27] S. Kim, C.B. Roth, J.M. Torkelson, Effect of nanoscale confinement on the glass transition temperature of free-standing polymer films: novel, self-referencing fluorescence method, J. Polym. Sci. B Polym. Phys. 46 (24) (2008) 2754–2764, https://doi.org/10.1002/polb.21591.
[28] J.H. Kim, J. Jang, W.C. Zin, Thickness dependence of the glass transition temperature in thin polymer films, Langmuir 17 (9) (2001) 2703–2710, https://doi.org/10.1021/la001125k.
[29] O. Tsui, T.P. Russell, C.J. Hawker, Effect of interfacial interactions on the glass transition of polymer thin films, Macromolecules 34 (16) (2001) 5535–5539, https://doi.org/10.1021/ma000028v.
[30] J.A. Forrest, K. Dalnoki-Veress, The glass transition in thin polymer films, Adv. Colloid Interface Sci. 94 (1–3) (2001) 167–196, https://doi.org/10.1016/S0001-8686(01)00060-4.
[31] T. Chikamatsu, M. Shahiduzzaman, K. Yamamoto, M. Karakawa, T. Kuwabara, K. Takahashi, T. Taima, Identifying molecular orientation in a bulk heterojunction film by infrared reflection absorption spectroscopy, ACS Omega 3 (5) (2018) 5678–5684, https://doi.org/10.1021/acsomega.8b00099.
[32] Y. Peng, Y. Liu, Q. Wu, P. Sun, Study on the glass transition process of polymer system using differential scanning calorimetry and fourier transform infrared spectroscopy, Anal. Sci. 33 (9) (2017) 1071–1076, https://doi.org/10.2116/analsci.33.1071.
[33] Y. Zhang, J.M. Zhang, Y.L. Lu, Y.X. Duan, S.K. Yan, D.Y. Shen, Glass transition temperature determination of poly(ethylene terephthalate) thin films using reflection-absorption FTIR, Macromolecules 37 (7) (2004) 2532–2537, https://doi.org/10.1021/ma035709f.
[34] O.N. Tretinnikov, K. Ohta, Conformation-sensitive infrared bands and conformational characteristics of stereoregular poly(methyl methacrylate)s by variable-temperature FTIR spectroscopy, Macromolecules 35 (19) (2002) 7343–7353, https://doi.org/10.1021/ma020411v.
[35] Y. Grohens, M. Brogly, C. Labbe, J. Schultz, Interfacial conformation energies of stereoregular poly(methyl methacrylate) by infra-red reflection absorption spectroscopy, Polymer 38 (24) (1997) 5913–5920, https://doi.org/10.1016/S0032-3861(97)00168-7.
[36] H.S. Shin, H. Lee, C.H. Jun, Y.M. Jung, S.B. Kim, Transition temperatures and molecular structures of poly(methyl methacrylate) thin films by principal component analysis: comparison of isotactic and syndiotactic poly(methyl methacrylate), Vib. Spectrosc. 37 (1) (2005) 69–76, https://doi.org/10.1016/j.vibspec.2004.06.005.
[37] H.S. Shin, Y.M. Jung, T.Y. Oh, T.Y. Chang, S.B. Kim, D.H. Lee, I. Noda, Glass transition temperature and conformational changes of poly(methyl methacrylate) thin films determined by a two-dimensional map representation of temperature-dependent reflection-absorption FTIR spectra, Langmuir 18 (15) (2002) 5953–5958, https://doi.org/10.1021/la020258y.

[38] Y.M. Jung, H.S. Shin, S.B. Kim, I. Noda, Two-dimensional gradient mapping technique useful for detailed spectral analysis of polymer transition temperatures, J. Phys. Chem. B 112 (12) (2008) 3611–3616, https://doi.org/10.1021/jp077043n.
[39] C.J. Ellison, J.M. Torkelson, The distribution of glass-transition temperatures in nanoscopically confined glass formers, Nat. Mater. 2 (10) (2003) 695–700, https://doi.org/10.1038/nmat980.
[40] C.J. Ellison, J.M. Torkelson, Sensing the glass transition in thin and ultrathin polymer films via fluorescence probes and labels, J. Polym. Sci. B Polym. Phys. 40 (24) (2002) 2745–2758, https://doi.org/10.1002/polb.10343.
[41] M.J. Burroughs, D. Christie, L.A.G. Gray, M. Chowdhury, R.D. Priestley, 21st century advances in fluorescence techniques to characterize glass-forming polymers at the nanoscale, Macromol. Chem. Phys. 219 (3) (2018) 1700368, https://doi.org/10.1002/macp.201700368.
[42] C.J. Ellison, S.D. Kim, D.B. Hall, J.M. Torkelson, Confinement and processing effects on glass transition temperature and physical aging in ultrathin polymer films: novel fluorescence measurements, Eur. Phys. J. E. 8 (2) (2002) 155–166, https://doi.org/10.1140/epje/i2001-10057-y.
[43] S. Kawana, R. Jones, Character of the glass transition in thin supported polymer films, Phys. Rev. E 63 (2) (2001), 021501, https://doi.org/10.1103/PhysRevE.63.021501.
[44] B. Hajduk, H. Bednarski, B. Trzebicka, Temperature-dependent spectroscopic ellipsometry of thin polymer films, J. Phys. Chem. B 124 (16) (2020) 3229–3251, https://doi.org/10.1021/acs.jpcb.9b11863.
[45] I. Karapanagiotis, D.F. Evans, W.W. Gerberich, Dewetting dynamics of thin polystyrene films from sputtered silicon and gold surfaces, Colloid. Surface. Physicochem. Eng. Aspect. 207 (1–3) (2002) 59–67, https://doi.org/10.1016/S0927-7757(02)00040-7.
[46] J. Peng, R. Xing, Y. Wu, B. Li, Y. Han, W. Knoll, D.H. Kim, Dewetting of thin polystyrene films under confinement, Langmuir 23 (5) (2007) 2326–2329, https://doi.org/10.1021/la061911a.
[47] P. Cao, P. Bai, A.A. Omrani, Y. Xiao, K.L. Meaker, H. Tsai, A. Yan, H.S. Jung, R. Khajeh, G.F. Rodgers, Y. Kim, A.S. Aikawa, M.A. Kolaczkowski, Y. Liu, A. Zettl, K. Xu, M.F. Crommie, T. Xu, Preventing thin film dewetting via graphene capping, Adv. Mater. 29 (36) (2017) 1701536, https://doi.org/10.1002/adma.201701536.
[48] X. Li, Y.C. Han, L. J, An, Inhibition of thin polystyrene film dewetting via phase separation, Polymer 44 (19) (2003) 5833–5841, https://doi.org/10.1016/S0032-3861(03)00585-8.
[49] G. Socrates, Infrared and Raman Characteristic Group Frequencies: Tables and Charts, John Wiley & Sons Ltd, England, 2001.
[50] D. Olmos, E.V. Martin, J. Gonzalez-Benito, New molecular-scale information on polystyrene dynamics in PS and PS-BaTiO3 composites from FTIR spectroscopy, Phys. Chem. Chem. Phys. 16 (44) (2014) 24339–24349, https://doi.org/10.1039/c4cp03516j.
[51] X. Liang, D. Huang, New insights into the effects of physical aging on glass transition of polystyrene by FTIR, J. Macromol. Sci. Part B-Phys. 51 (1–3) (2012) 348–357, https://doi.org/10.1080/00222348.2011.596796.
[52] Q. Yang, X. Chen, Z. He, F. Lan, H. Liu, The glass transition temperature measurements of polyethylene: determined by using molecular dynamic method, RSC Adv. 6 (15) (2016) 12053–12060, https://doi.org/10.1039/c5ra21115h.
[53] G. Reiter, Mobility of polymers in films thinner than their unperturbed size, Europhys. Lett. 23 (8) (1993) 579–584, https://doi.org/10.1209/0295-5075/23/8/007.
[54] V. Di Lisio, E. Sturabotti, I. Francolini, A. Piozzi, A. Martinelli, Application of temperature modulation to FTIR spectroscopy: an analysis of equilibrium and non-equilibrium conformational transitions of poly(ethylene terephthalate) in glassy and liquid states, J. Therm. Anal. Calorim.m. 142 (2020) 1835–1847, https://doi.org/10.1007/s10973-020-10169-0.
[55] V. Di Lisio, E. Sturabotti, I. Francolini, A. Piozzi, A. Martinelli, Effects of annealing above T-g on the physical aging of quenched PLLA studied by modulated temperature FTIR, J. Polym. Sci. B Polym. Phys. 57 (3) (2019) 174–181, https://doi.org/10.1002/polb.24769.
[56] V. Di Lisio, E. Sturabotti, I. Francolini, A. Piozzi, A. Martinelli, Isotactic polypropylene reversible crystallization investigated by modulated temperature and quasi-isothermal FTIR, J. Polym. Sci. B Polym. Phys. 57 (14) (2019) 922–931, https://doi.org/10.1002/polb.24847.